

High Accuracy Attitude Determination and Control of the DIVA Mission

Matthias Wiegand, Stephan Theil, Thomas Diedrich, Oliver Matthews

Center of Applied Space Technology and Microgravity, ZARM
University of Bremen, Germany

Abstract

Small satellite missions for scientific purpose gained more and more importance during the last years in Germany. There are several missions inorbit or scheduled for launch in the near future like GFZ (1995), Equator-S (inorbit, launch Dec 1997), ABRIXAS (launch April 1999) and other missions are on the horizon. One of these highly ambitious projects is the small astrometry satellite DIVA (German Interferometer for Multichannel Photometry and Astrometry). DIVA will be the successor of the HIPPARCOS satellite and a pathfinder to much larger missions like GAIA (Global Astrometric Interferometer for Astrophysics), FAME (Fizeau Astrometric Mapping Explorer) and SIM (Space Interferometry Mission). This work deals with the recent results from spacecraft dynamics simulations performed for the 150 kg DIVA satellite. The attitude determination requirements are quite ambitious for a small satellite mission, while the control requirements of 5 arcmin are moderate. The attitude determination system has to provide attitude information to the scientific payload with an accuracy of 1 arcsec in scan direction and 3 arcsec perpendicular to it using a Kalman filter that relies on attitude sensors and the scientific telescope. The scientific goal is a post mission scientific attitude accuracy of about 0.8 mas. The attitude control system relies on a cold gas system for first acquisition, safe mode and coarse attitude control. For fine attitude control the system is supported by utilizing the solar radiation pressure to minimize the thruster actions. Therefore, the solar panel alignment will be adjusted to support the nominal scanning law.

I. Introduction

This paper describes a Kalman filter algorithm for determining three-axis attitude of the DIVA mission. DIVA (Deutsches Interferometer für Vielkanalphotometrie und Astrometrie) is a small astronomical satellite planned by the Astronomisches Rechen-Institut, Heidelberg. The main scientific objective is to perform astrometric and photometric observations of at least four million stars.

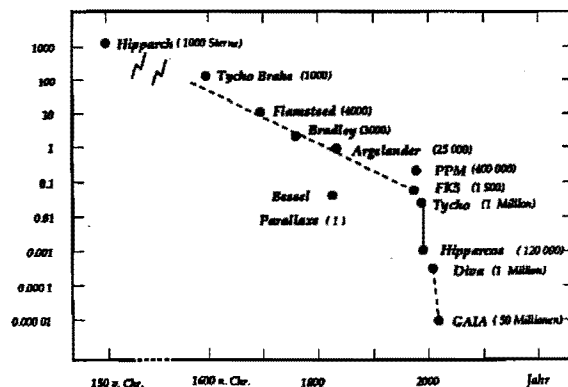


Figure 2: Accuracies of astrometric position measurements from Hipparch to GAIA

The mission is a successor of ESA's astrometry satellite HIPPARCOS (HIGH Precision Parallax Collecting Satellite). From 1989 to 1993 HIPPARCOS has measured positions of 120000 star within a mean accuracy of 1.5 mas. DIVA has also a precursor function for ESA's proposed GAIA (Global Astrometric Interferometer for Astrophysics) mission which aims to perform an astrometric survey at 10 microarcsec (μas). DIVA will measure parallaxes with an accuracy better than 0.6 milliarcseconds (mas) and proper motions better than 0.8 mas/yr for all stars brighter than $V=11$. The instrument simultaneously observes two fields of 0.5 degrees diameter each, separated by at least 60° on the sky.

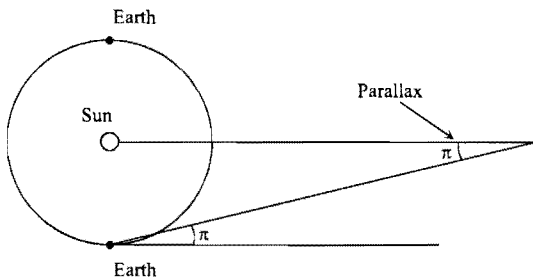


Figure 3: Parallax of stars. $\pi = 1$ arcsec means a distance of 1 Parsec

The optical configuration consists of two Fizeau interferometers with a baseline of 10 cm, one for each field of view. A beam combining mirror feeds light from both fields into a single modified Gregory telescope. A prism creates dispersed fringes from 400 to 900 nm in the focal plane. Light is recorded in the focal plane by a CCD mosaic operated in time-delayed integration mode, clocked synchronously with the satellite rotation. Additionally, broad-band photometric with a typical accuracy of 0.002 mag and multi-channel intermediate-band photometry with an accuracy 0.01 to 0.02 mag will be provided by DIVA.

To achieve the proposed precise parallax measurements real-time three-axis determination accuracy must be in the range of 1 arcsec. Thus, the attitude determination and control system is a major design driver.

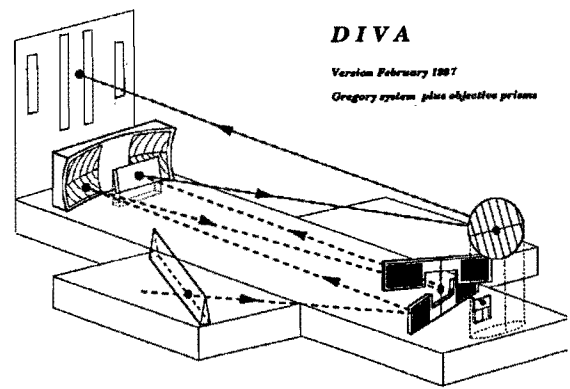


Figure 4: Schematic of the DIVA telescope

This work deals with the attitude determination and control system with special emphasis on attitude determination using a Kalman filter algorithm.

II. System Design Description

Figure 5 shows a rendered CAD drawing of the preliminary DIVA design. The outer shape is a truncated double cone of 112 cm diameter and 96 cm total height. Four solar panels (60 cm \times 80 cm) are mounted perpendicular to the symmetry axis. The instruments fits into a cylinder of 70 cm diameter and 45 cm height. The overall mass is approx 150 kg. The mean power consumption is 150 W.

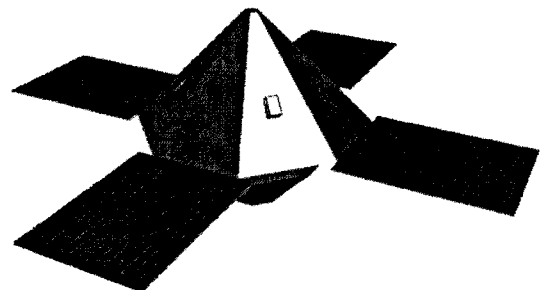


Figure 5: Diva Design

A geosynchronous orbit has been chosen to minimize external disturbances torques and eclipse durations over the two years mission. Launch is planned for 2002/03.

Scanning Law DIVA will scan the whole sky within 6 month. The scanning law is analogous to HIPPARCOS. The Z-axis (complies satellite symmetry axis) of the telescope reference frame (Figure 6) rotates at a constant angle $\xi = 45^\circ$ around the sun direction, following the sun in its apparent motion along the ecliptic and performing $K = 6.4$ revolutions per year. At the same time the satellite rotates around the Z-Axis with $1/80''/s$. The motions of the preceding and following telescope FOV, which scan the celestial sphere, result directly from this scanning motion.

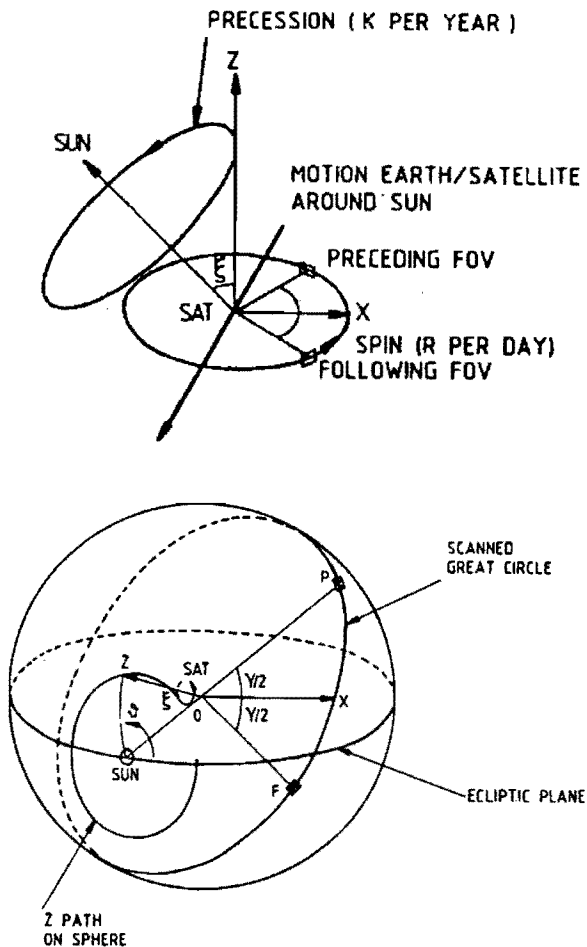


Figure 6: Definitions of the Telescope Reference Frame [9]

III. Attitude Determination and Control System

1. Requirements

Table 1 depicts the accuracy requirements for the nominal scanning law NSL.

only from star sensor	
three-axis accuracy	$5'' RMS$
control accuracy (attitude)	$\pm 5'$
star sensor plus scientific instrument	
accuracy in scan direction (w)	$\pm 1''$
accuracy \perp scan direction (z)	$\pm 3''$
rate accuracy (scan direction)	$\pm 0.1''/s$
rate accuracy (\perp scan direction)	$\pm 0.5''/s$
control accuracy (attitude)	$\pm 5'$
control accuracy (scan rate, w)	$\pm 4''/s$
control accuracy (scan rate, z)	$\pm 0.5''/s$

Table 1: Attitude Requirements

Issues concerning mechanical jitter of the structure due to disturbance torques are under investigation. Disturbance torques can be caused by the electromechanical and thermal environment as well as inaccuracies in the desired control torques.

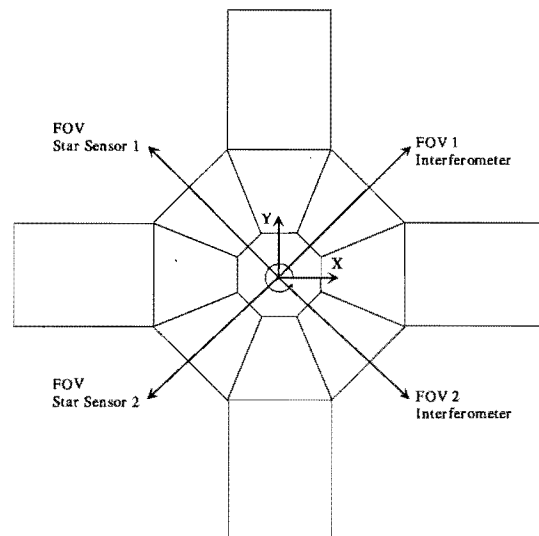


Figure 7: Star-Sensor and scientific instrument field of view

System Model	$\dot{\underline{x}}(t) = \underline{f}(\underline{x}(t), t) + \underline{w}(t)$
Measurement Model	$z_k = \underline{h}_k(\underline{x}(t_k)) + v_k, \quad k = 1, 2, \dots$
Assumptions	$\underline{w}(t) \sim N(\underline{0}, \underline{Q}(t)), v_k \sim N(0, \underline{R}_k), E[\underline{w}(t), v_k^T] = 0$
Initial Conditions	$\underline{x}(0) \sim N(\hat{\underline{x}}_0, \underline{P}_0)$
State Estimate Propagation	$\hat{\underline{x}}(t) = \underline{f}(\hat{\underline{x}}(t), t)$
Error Covariance Propagation	$\underline{P}(t) = \underline{F}(\hat{\underline{x}}(t), t)\underline{P}(t) + \underline{P}(t)\underline{F}^T(\hat{\underline{x}}(t), t) + \underline{Q}(t)$
State Estimate Update	$\hat{\underline{x}}_k(+)=\hat{\underline{x}}_k(-)+\underline{K}_k[z_k-\underline{h}_k(\hat{\underline{x}}_k(-))]$
Error Covariance Update	$\underline{P}_k(+)=\left[\underline{I}-\underline{K}_k\underline{H}_k(\hat{\underline{x}}_k(-))\right]\underline{P}_k(-)$
Gain Matrix	$\underline{K}_k=\frac{\underline{P}_k(-)\underline{H}_k^T(\hat{\underline{x}}_k(-))}{\left[\underline{H}_k(\hat{\underline{x}}_k(-))\underline{P}_k(-)\underline{H}_k^T(\hat{\underline{x}}_k(-))+\underline{R}_k\right]^{-1}}$
Definitions	$\underline{H}_k(\hat{\underline{x}}_k(-))\equiv\left.\frac{\partial\underline{h}_k(\underline{x})}{\partial\underline{x}}\right _{\underline{x}=\hat{\underline{x}}_k(-)}$ $\underline{F}(\hat{\underline{x}}(t), t)\equiv\left.\frac{\partial\underline{f}(\underline{x}(t), t)}{\partial\underline{x}(t)}\right _{\underline{x}(t)=\hat{\underline{x}}(t)}$

Table 2: Continuous-Discrete Extended Kalman Filter

2. ADCS Hardware

The attitude determination system relies primarily on the star-sensor and the scientific telescope itself. During safe mode and first acquisition sun-present, sun-sensor and gyros are used. During all modes control torquers are applied using a cold gas system (discontinuous control). However, if a continuous control becomes necessary electric propulsion system can be used. The control system is still under investigation. Figure 7 shows the alignment of the star-sensor and telescope field of views.

IV Filter Design

1. System State Vector

The system state vector \underline{x} is a seven-dimensional vector consisting of spacecraft attitude rate and attitude

$$\underline{x}^T = (\omega_x, \omega_y, \omega_z, q_1, q_2, q_3, q_4) \quad (1)$$

where the quaternion \underline{q} defines the transformation from the inertial frame to the body

frame. The attitude rate $\underline{\omega}$ is expressed in body coordinates.

The spacecraft attitude dynamics are modeled by the following equations

$$\dot{\underline{\omega}} = \underline{I}^{-1}[\underline{n} - \underline{\omega} \times \underline{I}\underline{\omega}] \quad (2)$$

$$\dot{\underline{q}} = \frac{1}{2}\underline{\tilde{\omega}} \otimes \underline{q} \quad (3)$$

where \underline{I} is the spacecraft inertia matrix and \underline{n} is the total external torque including disturbances and control torques. $\underline{\tilde{\omega}}$ denotes the quaternion representation of the angular velocity [1].

The state is propagated between updates according to the state equations (2) (3). The nonlinear equations are integrated using a fourth order Runge-Kutta method.

2. Filter State Vector

The Kalman Filter used for correcting the current attitude rate and attitude estimates has a six-dimensional filter state vector $\Delta\underline{x}$ given by

$$\begin{aligned}\Delta \underline{x}^T &= (\Delta \underline{\omega}^T, \Delta \underline{q}^T) \\ &= (\Delta \omega_x, \Delta \omega_y, \Delta \omega_z, \Delta q_1, \Delta q_2, \Delta q_3)\end{aligned}\quad (4)$$

where $\Delta \underline{\omega}$ is the rate error and $\Delta \underline{q}$ is a vector part of the attitude error quaternion $\Delta \underline{q}$ as defined in equation (5).

$$\begin{aligned}\Delta \underline{q} &= \left(\frac{\Delta \underline{q}}{\sqrt{1 - |\Delta \underline{q}|^2}} \right) \\ &= \begin{pmatrix} \Delta q_1 \\ \Delta q_2 \\ \Delta q_3 \\ \sqrt{1 - \Delta q_1^2 - \Delta q_2^2 - \Delta q_3^2} \end{pmatrix}\end{aligned}\quad (5)$$

Both parts of the filter state vector are defined by the following equation (6) where $\hat{\underline{q}}$ and $\hat{\underline{\omega}}$ are the current propagated attitude and attitude rate.

$$\begin{aligned}\underline{\omega} &= \hat{\underline{\omega}} + \Delta \underline{\omega} \\ \underline{q} &= \Delta \underline{q} \otimes \hat{\underline{q}}\end{aligned}\quad (6)$$

The state equation for the filter state vector \underline{x} resp. $\Delta \underline{\omega}$ and $\Delta \underline{q}$ can be derived using the attitude dynamics model and the definition of the filter state vector. The substitution of equations (6) into equations (2) and (3) yields the state equations for the filter state (7) and (8) (see [1]).

$$\begin{aligned}\Delta \dot{\underline{\omega}} &= \underline{I}^{-1} [\Delta \dot{\underline{m}} - \hat{\underline{\omega}} \times \underline{I} \Delta \underline{\omega} - \Delta \underline{\omega} \times \underline{I} \hat{\underline{\omega}} \\ &\quad - \Delta \underline{\omega} \times \underline{I} \Delta \underline{\omega}]\end{aligned}\quad (7)$$

$$\Delta \dot{\underline{q}} = \frac{1}{2} [\hat{\underline{\omega}} \otimes \Delta \underline{q} - \Delta \underline{q} \otimes \hat{\underline{\omega}} + \Delta \underline{\omega} \otimes \Delta \underline{q}]\quad (8)$$

3. Error Covariance Propagation

The error covariance propagation is performed for the filter state using the equation in table 2. The system matrix \underline{F} is defined as

$$\underline{F} = \underline{J}(\Delta \dot{\underline{x}}, \Delta \underline{x}) = \begin{bmatrix} \frac{\partial \Delta \dot{\omega}_x}{\partial \Delta \omega_x} & \dots & \frac{\partial \Delta \dot{\omega}_x}{\partial \Delta q_1} \\ \dots & \dots & \dots \\ \frac{\partial \Delta \dot{q}_1}{\partial \Delta \omega_x} & \dots & \frac{\partial \Delta \dot{q}_1}{\partial \Delta q_1} \end{bmatrix}\quad (9)$$

and can be derived using the equations (7) and (8).

4. Observation Model

The observations vector consists of three attitude angles provided by the star sensor and two tuples of attitude corrections provided by the scientific instrument. It is defined as follows

$$\underline{h}^T = (\alpha, \delta, \rho, \Delta w_1, \Delta z_1, \Delta w_2, \Delta z_2)\quad (10)$$

where α is the right ascension, δ the declination of the field of view of the star camera and ρ is the roll angle around the optical sensor axis. The coordinates w_i and z_i are CCD field coordinates of the interferometer where z is aligned with the body z axis and w is perpendicular to z and the optical axis. The index denotes the the field of view where the measurements have been taken.

As defined in table 2 the observation matrix \underline{H} is the partial derivative of the observable with respect to the filter state vector:

$$\begin{aligned}\underline{H} &= \underline{J}(\underline{h}, \Delta \underline{x}) \\ &= \begin{bmatrix} \frac{\partial h}{\partial \Delta \omega_x} & \dots & \frac{\partial h}{\partial \Delta q_1} \\ \dots & \dots & \dots \\ \mathbf{0}_{7 \times 3} & \dots & \frac{\partial h}{\partial \Delta q_1} \end{bmatrix}\end{aligned}\quad (11)$$

Due to the fact that the measurement model contains only vector or angle observable the partial derivative of the measurement model with respect to the attitude rate is zero.

The measurements of the interferometer have a mean update rate of $\frac{1}{4} Hz$ (worst case: Hipparcos star catalogue, scan perpendicular to milky way) but time spaces between measurements can be up to 20 seconds. To consider these measurements at

the time they were provided by the interferometer the observation matrix is modeled in the following way. The partial derivative of the field coordinates with respect to the attitude are set to zero if no measurement is provided.

5. Update

At the update times the sensor measurements are used to update the filter state $\Delta \underline{x}$. This is obtained using the equation in table 2. Then this updated filter state is used to correct the system state vector as defined in equation (6). After that the filter state vector is reinitialized to zero (12).

$$\Delta \underline{\omega} = 0, \quad \Delta \underline{q} = 0 \quad (12)$$

V Filter Performance

The first step to examine the filter performance is simulation testing. Thus several simulation tests have been done. Each test consists of four parts :

- Reference state and measurement calculation
- Adding noise to the measurements based on the assumed statistics
- Kalman filtering of the noisy measurements to obtain the best estimate
- Evaluation of results by comparison of best estimate and reference state

The attitude sensors for DIVA (star sensor, interferometer) have very different characteristics concerning accuracy and update rate. The star sensor accuracy is given by $\sigma_\alpha = \sigma_\delta = 6''$ for the attitude accuracy of the optical axis and $\sigma_\rho = 12''$ for the accuracy of the roll angle. The measurements are obtained at a rate of 1 Hz. For the scientific instrument a worst case for measurement accuracy was chosen assuming the Hipparcos star catalogue and a scan direction

perpendicular to the milky way. From that follows a measurement noise of $\sigma_{\Delta w} = 36mas$ and $\sigma_{\Delta z} = 890mas$. These values contain the error of the star catalogue and the CCD measurement error which depends of the star brightness. The calibration error is neglected. The mean rate of measurements for this case is $0.25Hz$. This rate was splitted for 2 fields of view into $0.125Hz$.

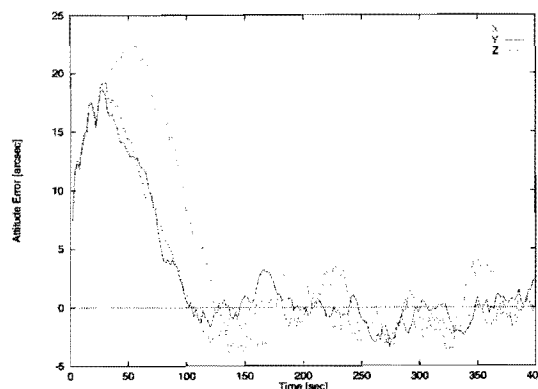


Figure 8: Transient State of Attitude Accuracy, Measurement Noise $\sigma_\alpha = \sigma_\delta = 6''$, $\sigma_\rho = 12''$, Measurement Update Rate $1Hz$, Sample Interval $1s$

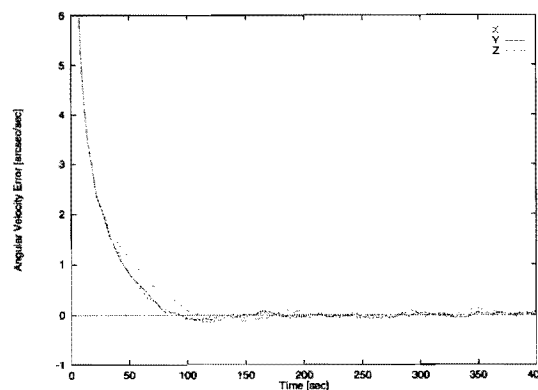


Figure 9: Transient State of Attitude Rate Accuracy, Measurement Noise $\sigma_\alpha = \sigma_\delta = 6''$, $\sigma_\rho = 12''$, Measurement Update Rate $1Hz$, Sample Interval $1s$

The figures 8 and 9 show the transient state of the attitude error and the attitude rate error. In this case only the star sensor is used for attitude determination. The first measurement of the star

sensor was used for deterministic attitude correction after that the Kalman Filter was started using the following measurements. So the initial error depends on the error of the first measurement.

Figure 10 shows the same simulation over a longer time span. In the steady state the attitude error is always smaller than $10''$ and has mean square value smaller than $5''$. So the accuracy of attitude determination meets the requirement listed in table 1.

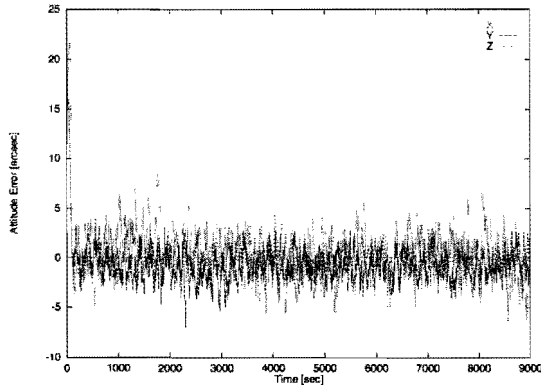


Figure 10: Steady State of Attitude Accuracy, Measurement Noise $\sigma_\alpha = \sigma_\delta = 6''$, $\sigma_\rho = 12''$, Measurement Update Rate $1Hz$, Sample Interval $1s$

Figure 11 shows the attitude error using the star sensor and one field of view of the scientific instrument. The instrument provides measurements in one field of view with a rate of $\frac{1}{4}Hz$ from a simulation time of $3200s$ on. So the attitude error decreases especially for the error of the rotation angle around the z axis because of the very small noise of the Δw measurements.

The full functionality is simulated by using the star sensor and the full scientific instrument for attitude determination. In this case the interferometer provide measurements in both field of views at an rate of $\frac{1}{4}Hz$. This simulation was simplified in the way that a measurement occur every 8 seconds per field of view. The figures 12 and 13 show the attitude and the attitude rate error for that case. Both error decrease enormously after invoking the scientific instrument for attitude determination. As it can be seen the attitude around

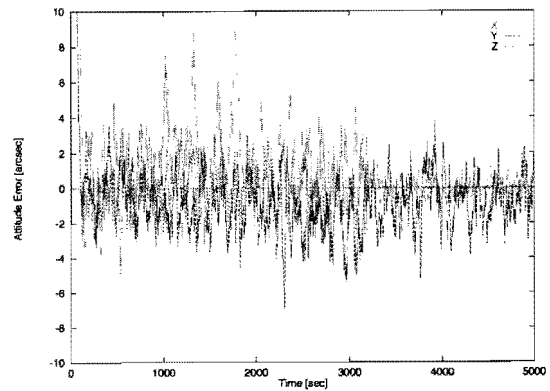


Figure 11: Attitude Accuracy using Star Sensor ($\sigma_\alpha = \sigma_\delta = 6''$, $\sigma_\rho = 12''$, $1Hz$) and the Scientific Instrument after $3200s$ (1 FOV, $\sigma_{\Delta w} = 36mas$, $\sigma_{\Delta z} = 890mas$, $0.25Hz$)

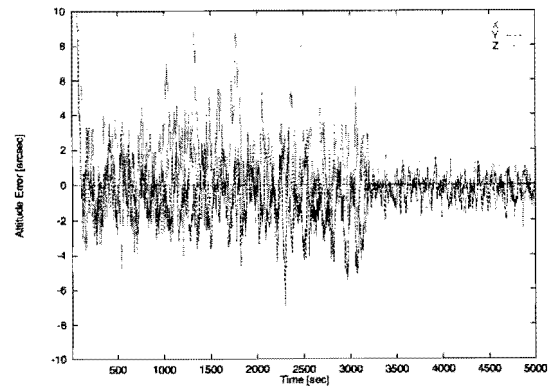


Figure 12: Attitude Accuracy using Star Sensor ($\sigma_\alpha = \sigma_\delta = 6''$, $\sigma_\rho = 12''$, $1Hz$) and the Scientific Instrument after $3200s$ (2 FOVs, $\sigma_{\Delta w} = 36mas$, $\sigma_{\Delta z} = 890mas$, $0.125Hz$ per FOV)

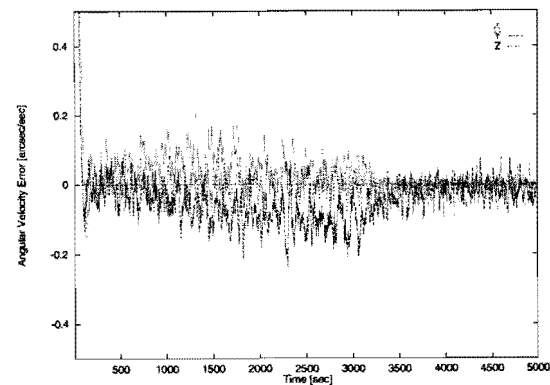


Figure 13: Attitude Accuracy using Star Sensor ($\sigma_\alpha = \sigma_\delta = 6''$, $\sigma_\rho = 12''$, $1Hz$) and the Scientific Instrument after $3200s$ (2 FOVs, $\sigma_{\Delta w} = 36mas$, $\sigma_{\Delta z} = 890mas$, $0.125Hz$ per FOV)

the z axis do not exceed 0.5" as well the attitude errors around the other axis are also smaller than the required limit. The root mean square values of attitude and rate error are significantly smaller than the requirements listed in table 1.

IV. Conclusion

It has been shown that the highly ambitious attitude determination requirements for the DIVA mission can be fulfilled on a cost-effective small space mission. Advanced filters help to reduce hardware costs while improving accuracy. The developed algorithms are ideally suited to combine the time variant measurements of both payload telescope field of views and the star-sensor. The accuracy relies strongly on the system dynamics model. Therefore, it is proposed to include the unmodeled torques in the attitude state in order to estimate the static portion by the Kalman filter. This will improve the filter performance in case of static unmodeled disturbance torques, i.e. residual magnetic dipole moments or unmodeled parts of the solar pressure. Issues concerning mechanical jitter of the structure are under investigation. These disturbances can be initiated thermally, electro-magnetically or as response to attitude control maneuvers.

Acknowledgments

This work has been performed under contract of Astronomisches Rechen-Institut ARI, Heidelberg, Germany as main contractor of the DLR founded DIVA study. We like to thank DLR and ARI for supporting our work.

References

- [1] Lefferts E. J. et al., "Kalman Filtering for Spacecraft Attitude Estimation", Journal of Guidance and Control, Vol. 5, Sep. 1982, pp. 417-429
- [2] Psiaki M. L. et al., "Three-Axis Attitude Determination via Kalman Filtering of Magnetometer Data", Journal of Guidance, Control and Dynamics, Vol. 13, May 1990, pp. 506-514
- [3] Martel F. et al., "Three-Axis Attitude Determination via Kalman Filtering of Magnetometer Data", Flight Mechanics/Estimation Theory Symposium, NASA Goddard Space Flight Center, Greenbelt Maryland, May 1988
- [4] Bak T., "Onboard Attitude Determination for a Small Satellite", 3rd International Conference on Spacecraft Guidance, Navigation and Control Systems, ESTEC, Noordwijk, The Netherlands, Nov. 1996
- [5] Gai E. et al., "Star-Sensor-Based Satellite Attitude/Attitude Rate Estimator", Journal of Guidance and Control, Vol. 8, April. 1985, pp. 560-565
- [6] Wertz J. R. (Ed.), "Spacecraft Attitude Determination and Control", D. Reidel Publishing Company, Boston, 1978
- [7] Jazwinski A. H., "Stochastic Processes and Filtering Theory", Vol. 64 of Mathematics in Science and Engineering, Academic Press, London, 1970
- [8] Gelb, A. (Ed.), "Applied Optimal Estimation", The M.I.T. Press, Cambridge, Massachusetts, 1974
- [9] PERRYMAN, M.A.C., ET. AL., "The Hipparcos Mission Pre-launch Status", Volume I, ESA SP-1111, 1989